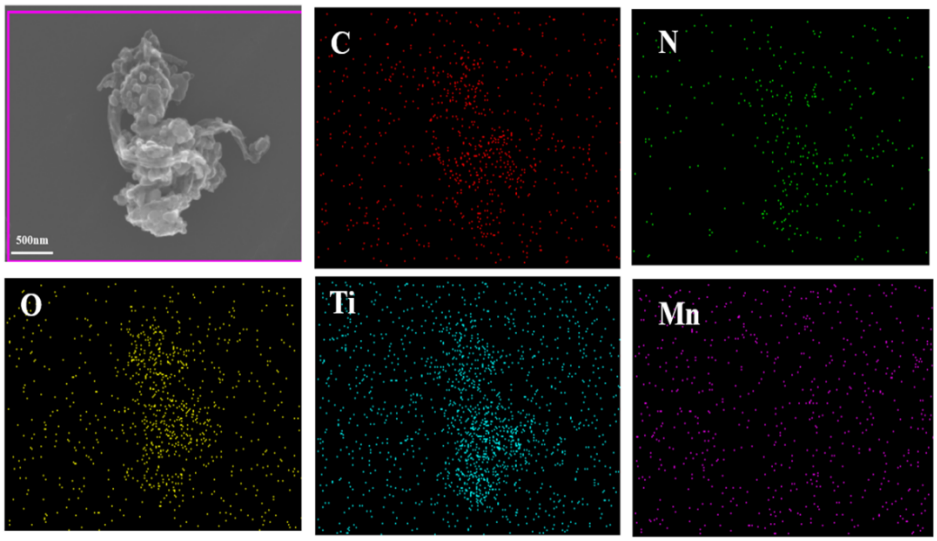

Fig. S1 Elemental mapping image of MnO/TiO_2/C/N-CNTs.

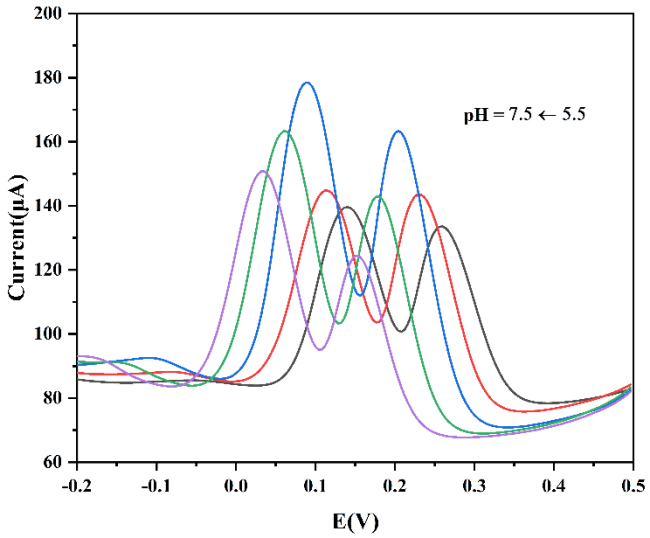

Fig. S2 The changes of oxidation peak current and potential of CC and HQ at different pH values

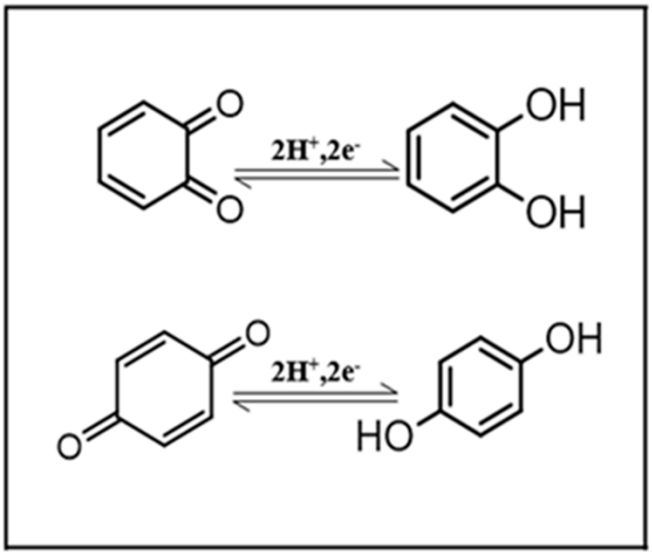

Fig. S3 Principles of CC and HQ reactions at $MnO/TiO_2/C/N$-CNTs/GCE surface.

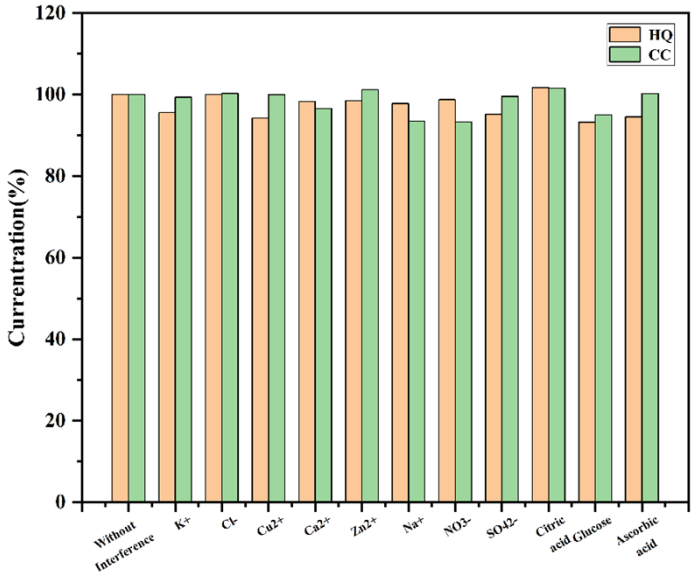

Fig. S4 Effects of different interfering substances on the detection of CC and HQ at $MnO/TiO_2/C/N$-CNTs/GCE.

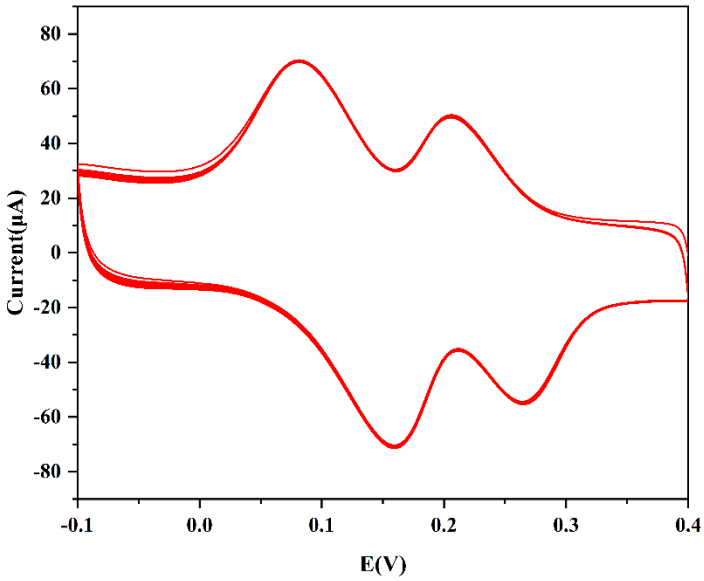

Fig. S5 CV curves of MnO/TiO_2/C/N-CNTs/GCE were scanned in 0.1 M PBS containing 50 μM CC and 50 μM HQ for 50 consecutive cycles.

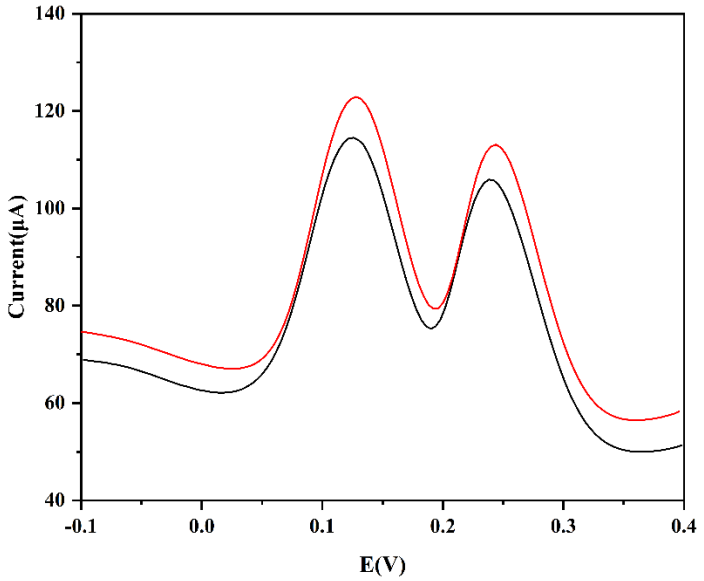

Fig. S6 DPV curves of CC and HQ at the MnO/TiO2/C/N-CNTs/GCE before and after 7 days of storage at 4 °C in a refrigerator.

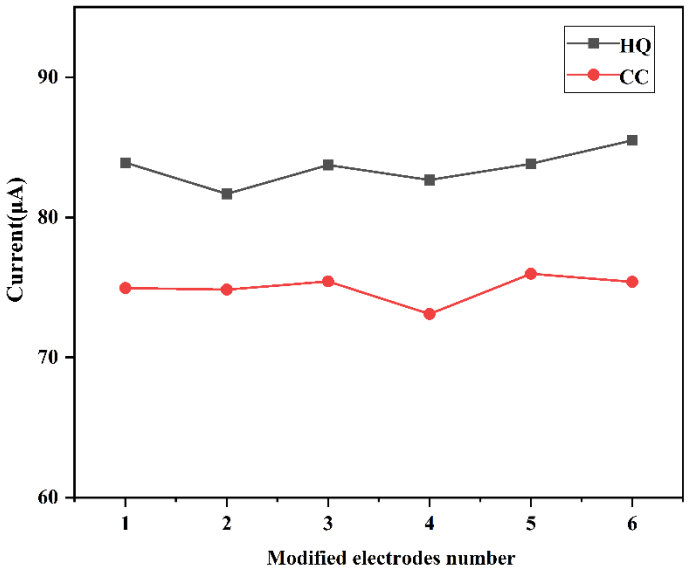

Fig. S7 DPV response currents of the six modified electrodes to CC and HQ.